Generalized Frequency Modulation

Wade P. Torres, Alan V. Oppenheim, and Rodolfo Ruben Rosales

***Abstract*—A generalization of frequency modulation is developed in which state trajectories of dynamical systems are used as carrier waves. Our focus is on the design and analysis of modulators and demodulators for such generalized frequency modulation systems. In particular, we show that for a class of dynamical systems, among which are certain chaotic systems, it is possible to develop a general approach to demodulation. This approach to demodulation results in a systematic procedure for demodulator construction that depends on the underlying dynamical system in a simple manner.**

***Index Terms*—Chaos, communications, frequency modulation, nonlinear oscillators.**

I. Introduction

THIS paper presents an approach to information transmission that can be viewed as a generalization of frequency modulation. The approach is based on modulating the rate of evolution of a dynamical system that has a periodic, almost periodic or chaotic trajectory and has a known exponentially convergent observer. Volkovskii [1] also noted that a chaotic system can be modulated by varying the time-constant of the system. In that work, the method of demodulation considered phase-locks by adjusting the time-constant according to phase differences in Poincare crossings. Our demodulator capitalizes on the characteristics of the observer and is based on a perturbation expansion of the observer error.

Among the dynamical systems to which our approach can be applied are those with sinusoidal solutions, and as we show, applying our modulation scheme to these systems produces waveforms identical to those found in traditional FM systems. Another class are chaotic systems that have the self-synchronizing property [2]. More generally, our approach can be applied to chaotic dynamical systems for which the observer may not be a self-synchronizing replica system.

The next section of this paper describes the modulation procedure and its relation to traditional FM. Sections III, IV, and V focus on a general approach to constructing demodulators. In particular, we develop an approach to demodulator construction that is independent of the underlying dynamical system, yielding a systematic demodulator design procedure. Specific examples of demodulation are given for the cases in which the underlying dynamical systems are the Van der Pol oscillator and the chaotic Lorenz system. In Section VI, some experimental results are presented that demonstrate the robustness in the presence of additive noise. Section VII describes a hardware implementation of a modulator and demodulator based on the chaotic Lorenz system.

Manuscript received March 8, 2001; revised August 14, 2001. The work of W. Torres and A. Oppenheim was supported in part by the Advanced Sensors Collaborative Technology Alliance, United States Army Research Laboratory under Grant DAAD19-01-2-0008. The work of W. Torres supported in part by the AT&T Labs Fellowship Program. The work of R. Rosales was supported in part by the National Science Foundation under Grant DMS-9802713. This paper was recommended by Guest Editor L. Kocarev.

W. Torres and A. Oppenheim are with the Research Laboratory of Electronics, Massachusetts Institute of Technology, Cambridge, MA 02139 USA.

R. Rosales is with the Department Mathematics, Massachusetts Institute of Technology, Cambridge, MA 02139 USA.

Publisher Item Identifier S 1057-7122(01)10382-X.

II. Modulation

An information signal, $m(t)$, is modulated onto a carrier wave by modulating the rate at which a dynamical system evolves. The dynamical system is represented in state-space form as

$$\begin{aligned}\dot{\mathbf{x}} &= \mathbf{f}(\mathbf{x})\\ y &= h(\mathbf{x})\end{aligned} \tag{1}$$

where $\mathbf{x} = [x_1\ x_2\ \cdots\ x_N]^T$ is an N-dimensional vector and the transmitted signal, y, is chosen as a scalar function of the state variables. The corresponding modulation system is

$$\begin{aligned}\dot{\mathbf{x}} &= (\omega_c + \beta m(t))\mathbf{f}(\mathbf{x})\\ y &= h(\mathbf{x})\end{aligned} \tag{2}$$

where ω_c is the *carrier rate* and β is the *modulation gain*. We assume throughout that β is chosen such that $|\beta m(t)| < \omega_c$ for all t.

To see the effect of introducing modulation, let $\mathbf{x}_{\rm nom}(t)$ represent a solution to the nominal system given in (1) and $\mathbf{x}_{\rm mod}(t)$ represent a solution to the modulated system given in (2). The two solutions are related by

$$\mathbf{x}_{\rm mod}(t) = \mathbf{x}_{\rm nom}\left(\omega_c t + \beta\int_0^t m(\tau)\,d\tau\right). \tag{3}$$

This relationship can be validated by first differentiating both sides of (3) with respect to t, which gives

$$\begin{aligned}\dot{\mathbf{x}}_{\rm mod} &= (\omega_c + \beta m(t))\mathbf{f}\left(\mathbf{x}_{\rm nom}\left(\omega_c t + \beta\int_0^t m(\tau)\,d\tau\right)\right)\\ &= (\omega_c + \beta m(t))\mathbf{f}(\mathbf{x}_{\rm mod}).\end{aligned} \tag{4}$$

Therefore

$$\mathbf{x}_{\rm mod}(t) = \mathbf{x}_{\rm nom}\left(\omega_c t + \beta\int_0^t m(\tau)\,d\tau\right) \tag{5}$$

is a solution to (2). Assuming $\mathbf{f}(\mathbf{x})$ and $m(t)$ are continuous, (1) and (2) both have unique solutions. If $\mathbf{x}_{\rm nom}(0) = \mathbf{x}_{\rm mod}(0)$, then $\mathbf{x}_{\rm nom}(t)$ given in (5) is the solution to (2). A block diagram of the complete modulation system is shown in Fig. 1.

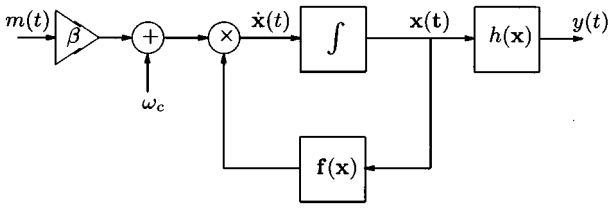

Fig. 1. A block diagram of the modulator.

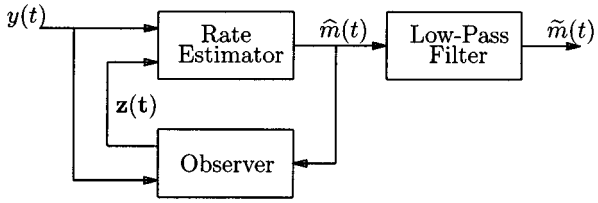

Fig. 2. A block diagram of the basic demodulator structure. The signal $y(t)$ is the transmitted signal, $\hat{m}(t)$ is the estimate of the modulating signal, and $\mathbf{z}(t)$ is the estimate of state variables of the transmitter system.

When one of the state-space solutions, x_i, of (1) follows a sinusoidal trajectory and that component is the transmitted signal, it follows from (3) that

$$x_i(t) = y(t) = \sin\left(\omega_c t + \int_0^t m(\tau)\,d\tau + \theta_0\right) \tag{6}$$

which is the same type of signal transmitted in traditional FM.

III. Demodulation

One of the requirements we impose on the dynamical system is that it have a known exponentially convergent observer. Exploiting this condition, we develop a systematic procedure for constructing demodulators.

A. Demodulator Structure

The basic demodulator structure is shown in Fig. 2. The observer is assumed to be known. The rate estimator is designed so that its interconnection with the observer, as depicted in the figure, results in an overall system that demodulates the transmitted signal to recover $m(t)$. The low-pass filter removes any spectral energy known to be absent from the original modulating signal, $m(t)$. Since this filter does not affect the convergence properties of the demodulator, it is not included in the analysis of this section.

The observer is represented by the dynamical state equation

$$\dot{\mathbf{z}} = \hat{\mathbf{f}}(\mathbf{z}, y) \tag{7}$$

where y is the output of (1). We assume that the observer is exponentially convergent, i.e., the state vector, $\mathbf{z}$, converges exponentially to the state, $\mathbf{x}$, of the nominal system in (1). It is worth noting and useful shortly that

$$\mathbf{f}(\mathbf{x}) = \hat{\mathbf{f}}(\mathbf{x}, y). \tag{8}$$

This follows from the fact that if $\mathbf{z} = \mathbf{x}$, then the observer is and remains synchronized, in which case $\dot{\mathbf{z}} = \dot{\mathbf{x}}$.

As depicted in the figure, the rate estimator has as inputs the transmitted signal, $y(t)$, and the observer's state estimate, $\mathbf{z}$. The entire modulation/demodulation system is represented as

$$\begin{aligned} \text{Modulator: } &\begin{cases} \dot{\mathbf{x}} = (\omega_c + \beta m)\mathbf{f}(\mathbf{x}) \\ y = h(\mathbf{x}) \end{cases} \\ \text{Demodulator: } &\begin{cases} \dot{\mathbf{z}} = (\omega_c + \beta \hat{m})\hat{\mathbf{f}}(\mathbf{z}, y) \\ \hat{m} = \mathcal{G}(\mathbf{z}, y), \end{cases} \end{aligned} \tag{9}$$

where $\mathcal{G}$ is the operator that represents the rate estimator.

B. Rate Estimator Design Based on a "Backward" Perturbation Expansion

We begin by assuming that the modulating signal is an unknown constant, i.e., $m(t) = m_0$. If the demodulator converges to both the transmitter state and to the constant modulating signal, then we assume that as long as $m(t)$ varies sufficiently slowly, the demodulator will track a time-varying $m(t)$.

To make the system shown in Fig. 2 converge to both $\mathbf{x}$ and m_0, we use a novel technique we refer to as a "backward" perturbation expansion. In the expansion, we express the modulator state, $\mathbf{x}$, as a perturbation expansion about the demodulator state, $\mathbf{z}$, in terms of the rate error, $e_m = \hat{m} - m_0$. Although expanding the drive system in terms of the response system may seem unusual, it is the key step in determining a rate estimator system that results in a convergent demodulator system.

The perturbation expansion has the form

$$\mathbf{x} = \boldsymbol{\xi}_0 + e_m\boldsymbol{\xi}_1 + e_m^2\boldsymbol{\xi}_2 + \cdots. \tag{10}$$

To show that this expansion is valid and that $\boldsymbol{\xi}_0 = \mathbf{z}$, we first differentiate both sides of (10), resulting in

$$\begin{aligned} &\dot{\boldsymbol{\xi}}_0 + e_m\dot{\boldsymbol{\xi}}_1 + \dot{e}_m\boldsymbol{\xi}_1 + \cdots \\ &\quad = (\omega_c + \beta m_0)\mathbf{f}(\mathbf{x}) \\ &\quad = (\omega_c + \beta m_0)\hat{\mathbf{f}}\left(\boldsymbol{\xi}_0 + e_m\boldsymbol{\xi}_1 + e_m^2\boldsymbol{\xi}_2 + \ldots, y\right) \\ &\quad = (\omega_c + \beta(\hat{m} - e_m))\hat{\mathbf{f}}\left(\boldsymbol{\xi}_0 + e_m\boldsymbol{\xi}_1 + e_m^2\boldsymbol{\xi}_2 + \ldots, y\right). \end{aligned} \tag{11}$$

In (11), we have used (2) and the fact that $\mathbf{f}(\mathbf{x}) = \hat{\mathbf{f}}(\mathbf{x}, y)$ according (8). Expanding $\hat{\mathbf{f}}(\cdot,\cdot)$ in a Taylor series gives

$$\begin{aligned} &\dot{\boldsymbol{\xi}}_0 + e_m\dot{\boldsymbol{\xi}}_1 + \dot{e}_m\boldsymbol{\xi}_1 + \cdots \\ &\quad = (\omega_c + \beta\hat{m})\hat{\mathbf{f}}(\boldsymbol{\xi}_0, y) + (\omega_c + \beta\hat{m})\frac{\partial\hat{\mathbf{f}}}{\partial\boldsymbol{\xi}_0}(\boldsymbol{\xi}_0, y)e_m\boldsymbol{\xi}_1 \\ &\qquad - \beta\hat{\mathbf{f}}(\boldsymbol{\xi}_0, y)e_m + \cdots. \end{aligned} \tag{12}$$

We now assume that $\dot{e}_m$ is of the form

$$\dot{e}_m = -Kr(\boldsymbol{\xi}_0, \boldsymbol{\xi}_1)e_m \tag{13}$$

where $r(\cdot,\cdot) : \mathbb{R}^{2N} \to \mathbb{R}$. Equating terms of equal power in e_m and neglecting terms of higher order than first, we are left with two equations, specifically

$$\dot{\boldsymbol{\xi}}_0 = (\omega_c + \beta\hat{m})\hat{\mathbf{f}}(\boldsymbol{\xi}_0, y) \tag{14}$$

and

$$\dot{\boldsymbol{\xi}}_1 = \left((\omega_c + \beta\hat{m})\frac{\partial\hat{\mathbf{f}}}{\partial\boldsymbol{\xi}_0}(\boldsymbol{\xi}_0, y) + Kr(\boldsymbol{\xi}_0, \boldsymbol{\xi}_1)\right)\boldsymbol{\xi}_1 - \beta\hat{\mathbf{f}}(\boldsymbol{\xi}_0, y). \tag{15}$$

Note that (14) implies that $\boldsymbol{\xi}_0 = \mathbf{z}$. The perturbation expansion is valid if $\boldsymbol{\xi}_1$ is bounded. We next show that the assumption that the observer is exponentially convergent leads to a bounded $\boldsymbol{\xi}_1$.

The error equation for the transmitter/observer coupling for the case in which there is no modulation is

$$\begin{aligned}\dot{\mathbf{e}}_\mathbf{z} &= \omega_c(\hat{\mathbf{f}}(\mathbf{e}_\mathbf{z}+\mathbf{x},y)-\hat{\mathbf{f}}(\mathbf{x},y))\\ &= \omega_c(\hat{\mathbf{f}}(\mathbf{z},y)-\hat{\mathbf{f}}(\mathbf{z}-\mathbf{e}_\mathbf{z},y)).\end{aligned} \tag{16}$$

The assumption that the observer is exponentially stable is equivalent to (16) having an exponentially stable equilibrium point at $\mathbf{e}_\mathbf{z} = \mathbf{0}$. A nonlinear system has an exponentially stable equilibrium point at $\mathbf{e}_\mathbf{z} = \mathbf{0}$ if and only if the corresponding linearized system has an exponentially stable equilibrium point at $\mathbf{e}_\mathbf{z} = \mathbf{0}$ [3]. Therefore, the system given by

$$\dot{\mathbf{e}}_\mathbf{z} = \omega_c \frac{\partial \hat{\mathbf{f}}}{\partial \mathbf{z}}(\mathbf{z},y)\mathbf{e}_\mathbf{z} \tag{17}$$

has an exponentially stable equilibrium point at $\mathbf{e}_\mathbf{z} = \mathbf{0}$. As long as $\omega_c + \beta\hat{m} > 0$

$$\dot{\mathbf{e}}_\mathbf{z} = (\omega_c + \beta\hat{m})\frac{\partial \hat{\mathbf{f}}}{\partial \mathbf{z}}(\mathbf{z},y)\mathbf{e}_\mathbf{z} \tag{18}$$

also has an exponentially stable equilibrium point at $\mathbf{e}_\mathbf{z} = \mathbf{0}$. The perturbed system given by

$$\dot{\mathbf{e}}_\mathbf{z} = (\omega_c + \beta\hat{m})\frac{\partial \hat{\mathbf{f}}}{\partial \mathbf{z}}(\mathbf{z},y)\mathbf{e}_\mathbf{z} + Kr(\mathbf{z},\mathbf{e}_\mathbf{z}) \tag{19}$$

is also exponentially stable provided that

$$\frac{\|r(\mathbf{z},\mathbf{e}_\mathbf{z})\|}{\|\mathbf{e}_\mathbf{z}\|} < \gamma \tag{20}$$

for some constant $\gamma > 0$ and $0 < K < K_*$ for some sufficiently small K_* [3]. An exponentially stable linear system is bounded input-bounded output (BIBO) stable [4]. Since $\hat{\mathbf{f}}(\mathbf{z},y)$ is bounded

$$\dot{\mathbf{e}}_\mathbf{z} = \left((\omega_c + \beta\hat{m})\frac{\partial \hat{\mathbf{f}}}{\partial \mathbf{z}}(\mathbf{z},y) + Kr(\mathbf{z},\mathbf{e}_\mathbf{z})\right)\mathbf{e}_\mathbf{z} - \beta\hat{\mathbf{f}}(\mathbf{z},y) \tag{21}$$

results in a bounded $\mathbf{e}_\mathbf{z}$. But (21) is identical to (15), which means $\boldsymbol{\xi}_1$ is bounded and the perturbation expansion is valid. Notice that $\boldsymbol{\xi}_1$ is determined by $\mathbf{z}, y$, and $\hat{m}$, all of which are signals that are local to the demodulator. We now show how the perturbation variable, $\boldsymbol{\xi}_1$, can be used to force $\hat{m}$ to converge to m_0.

The perturbation expansion can be used to approximate, to first-order, the difference between $y = h(\mathbf{x})$ and $\hat{y} = h(\mathbf{z})$ as

$$\begin{aligned}\hat{y} - y &= h(\mathbf{z}) - h(\mathbf{x})\\ &= h(\mathbf{z}) - h(\mathbf{z} + e_m\boldsymbol{\xi}_1 + \cdots)\\ &= -\frac{\partial h}{\partial \mathbf{z}}(\mathbf{z})\cdot\boldsymbol{\xi}_1 e_m + \mathcal{O}\left(e_m^2\right).\end{aligned} \tag{22}$$

Since $\boldsymbol{\xi}_1$ can be generated in the demodulator, we can choose $\hat{m}$ to be

$$\dot{\hat{m}} = K(\hat{y}-y)g\left(\frac{\partial h}{\partial \mathbf{z}}(\mathbf{z})\cdot\boldsymbol{\xi}_1\right) \tag{23}$$

where $g(\cdot)$ is a real-valued function that has the property $\operatorname{sgn}(g(a)) = \operatorname{sgn}(a)$, i.e., $g(\cdot)$ has the same sign as its argument. This gives, to first-order,

$$\begin{aligned}\dot{\hat{m}} &= -K\left(\frac{\partial h}{\partial \mathbf{z}}(\mathbf{z})\cdot\boldsymbol{\xi}_1\right)\cdot g\left(\frac{\partial h}{\partial \mathbf{z}}(\mathbf{z})\cdot\boldsymbol{\xi}_1\right)e_m\\ \dot{\hat{m}} &= -K\left(\frac{\partial h}{\partial \mathbf{z}}(\mathbf{z})\cdot\boldsymbol{\xi}_1\right)\cdot g\left(\frac{\partial h}{\partial \mathbf{z}}(\mathbf{z})\cdot\boldsymbol{\xi}_1\right)(\hat{m}-m_0).\end{aligned} \tag{24}$$

To clarify the behavior of $\hat{m}$, we write its equation of motion as

$$\dot{\hat{m}} = a(t)(\hat{m} - m_0) \tag{25}$$

where the time-varying coefficient, $a(t)$, is

$$a(t) = -K\left(\frac{\partial h}{\partial \mathbf{z}}(\mathbf{z})\cdot\boldsymbol{\xi}_1\right)\cdot g\left(\frac{\partial h}{\partial \mathbf{z}}(\mathbf{z})\cdot\boldsymbol{\xi}_1\right) \le 0 \tag{26}$$

and $a(t) = 0$ only when $h(\mathbf{x}) = h(\mathbf{z})$. Since $a(t)$ is negative for nonzero error, $\hat{m}$ converges to m_0 exponentially. It follows that $\mathbf{z}$ converges to $\mathbf{x}$ exponentially as well. Our earlier assumption that

$$\dot{e}_m = -Kr(\mathbf{z},\boldsymbol{\xi}_1)e_m \tag{27}$$

is valid with

$$r(\mathbf{z},\boldsymbol{\xi}_1) = \left(\frac{\partial h}{\partial \mathbf{z}}(\mathbf{z})\cdot\boldsymbol{\xi}_1\right)\cdot g\left(\frac{\partial h}{\partial \mathbf{z}}(\mathbf{z})\cdot\boldsymbol{\xi}_1\right). \tag{28}$$

Also, $g(\cdot)$ must be chosen so that $r(\cdot)$ satisfies (20).

C. Demodulator Summary

Given an exponentially convergent observer, $\hat{\mathbf{f}}(\cdot,\cdot)$, of the nominal system given in (1), a convergent demodulator can be constructed as

$$\begin{aligned}\dot{\mathbf{z}} &= (\omega_c + \beta\hat{m})\hat{\mathbf{f}}(\mathbf{z},y)\\ \hat{y} &= h(\mathbf{z})\\ \dot{\hat{m}} &= K(\hat{y}-y)g\left(\frac{\partial h}{\partial \mathbf{z}}(\mathbf{z})\cdot\boldsymbol{\xi}_1\right)\\ \dot{\boldsymbol{\xi}}_1 &= \left((\omega_c + \beta\hat{m})\frac{\partial \hat{\mathbf{f}}}{\partial \mathbf{z}}(\mathbf{z},y) + Kr(\mathbf{z},\boldsymbol{\xi}_1)\right)\boldsymbol{\xi}_1 - \beta\mathbf{f}(\mathbf{z},y)\end{aligned} \tag{29}$$

where

$$r(\mathbf{z},\boldsymbol{\xi}_1) = \left(\frac{\partial h}{\partial \mathbf{z}}(\mathbf{z})\cdot\boldsymbol{\xi}_1\right)\cdot g\left(\frac{\partial h}{\partial \mathbf{z}}(\mathbf{z})\cdot\boldsymbol{\xi}_1\right) \tag{30}$$

$0 < K < K_*$ for some K_*, and $g : \mathbb{R} \to \mathbb{R}$ such that $\operatorname{sgn}(g(a)) = \operatorname{sgn}(\mathrm{a})$ and $r(\cdot,\cdot)$ satisfies (20).

Explicit determination of K_* requires knowledge of a Lyapunov function for the linear, time-varying system given by

$$\dot{\boldsymbol{\xi}}_1 = \frac{\partial \hat{\mathbf{f}}}{\partial \mathbf{x}}(\mathbf{x},y)\boldsymbol{\xi}_1 \tag{31}$$

which is generally difficult to determine. K_* can also be determined by computing the Floquet exponents (for periodic systems) [4] or the Lyapunov exponents (for aperiodic systems) [5].

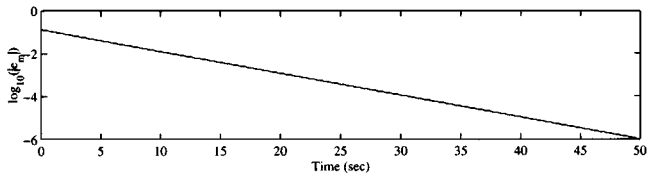

Fig. 3. Convergence of the rate estimate for the Van der Pol based system with $K = 1$ and $\beta = 1$.

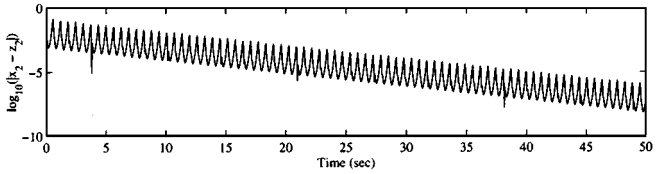

Fig. 4. The convergence of the state estimate for the Van der Pol based system with $K = 1$ and $\beta = 1$.

IV. Demodulator Examples

In this section, we demonstrate the modulation and demodulation scheme for two different dynamical systems. The first is based on the Van der Pol oscillator, which is a two-dimensional nonlinear system with a periodic attractor. The second system is the Lorenz system, which is a chaotic system with a strange attractor.

A. The Van der Pol Oscillator

The differential equation describing the Van der Pol oscillator is

$$\begin{aligned} \dot{x}_1 &= x_2 \\ \dot{x}_2 &= \lambda\left(1 - x_1^2\right) x_2 - x_1 \end{aligned} \tag{32}$$

where $\lambda > 0$. An exponentially convergent observer of the Van der Pol oscillator is

$$\begin{aligned} \dot{z}_1 &= z_2 + y - z_1 \\ \dot{z}_2 &= \lambda(1 - y^2) z_2 - y. \end{aligned} \tag{33}$$

Introducing modulation into (32) and following the formulation specified in (29), the modulator and demodulator are

$$\begin{aligned} &\underline{\text{Modulator}} \\ &\dot{x}_1 = (\omega_c + \beta m) x_2 \\ &\dot{x}_2 = (\omega_c + \beta m)\left(\lambda\left(1 - x_1^2\right) x_2 - x_1\right) \\ &y = x_1 \\ &\underline{\text{Demodulator}} \\ &\dot{z}_1 = (\omega_c + \beta \hat{m})(z_2 + y - z_1) \\ &\dot{z}_2 = (\omega_c + \beta \hat{m})(\lambda(1 - y^2) z_2 - y) \\ &\hat{y} = z_1 \\ &\dot{\hat{m}} = K(\hat{y} - y)\operatorname{sgn}(\psi_1) \\ &\begin{bmatrix} \dot{\psi}_1 \\ \dot{\psi}_2 \end{bmatrix} = \left((\omega_c + \beta \hat{m}) \begin{bmatrix} -1 & 1 \\ 0 & \lambda(1 - y^2) \end{bmatrix} + KIr(\mathbf{z}, \psi)\right) \\ &\qquad \times \begin{bmatrix} \psi_1 \\ \psi_2 \end{bmatrix} - \beta \begin{bmatrix} z_2 + y - z_1 \\ \lambda(1 - y^2) z_2 - y \end{bmatrix} \end{aligned} \tag{34}$$

where I is the 2×2 identity matrix and

$$r(\mathbf{z}, \psi) = |\psi_1|. \tag{35}$$

The convergence of $\hat{m}$ when $K = 1, \lambda = 1$, and $\beta = 1$ is shown in Fig. 3. The convergence of the state variable z_2 to x_2 is shown in Fig. 4. The numerical simulations in this paper were done using Matlab's ODE suite with a relative tolerance of 10^{-4} and an absolute tolerence of 10^{-7}.

B. The Lorenz System

The next example uses the Lorenz system for the underlying dynamical system. The Lorenz system is an example of a chaotic system, which is characterized by long-term aperiodic signals and a sensitive dependence on initial conditions. The Lorenz equations are

$$\begin{aligned} \dot{x}_1 &= \sigma(x_2 - x_1) \\ \dot{x}_2 &= r x_1 - x_1 x_3 - x_2 \\ \dot{x}_3 &= x_1 x_2 - b x_3 \end{aligned} \tag{36}$$

where $\sigma = 10, r = 25$, and $b = 8/3$. An exponentially convergent observer of this system is

$$\begin{aligned} \dot{z}_1 &= \sigma(z_2 - z_1) \\ \dot{z}_2 &= r y - y z_3 - z_2 \\ \dot{z}_3 &= y z_2 - b z_3. \end{aligned} \tag{37}$$

Adding the modulation to (36) and following the formulation specified in (29), the complete Lorenz-based modulation/demodulation system is given by

$$\begin{aligned} &\underline{\text{Modulator}} \\ &\dot{x}_1 = (\omega_c + \beta m)\sigma(x_2 - x_1) \\ &\dot{x}_2 = (\omega_c + \beta m)(r x_1 - x_1 x_3 - x_2) \\ &\dot{x}_3 = (\omega_c + \beta m)(x_1 x_2 - b x_3) \\ &y = x_1 \\ &\underline{\text{Demodulator}} \\ &\dot{z}_1 = (\omega_c + \beta \hat{m})\sigma(z_2 - z_1) \\ &\dot{z}_2 = (\omega_c + \beta \hat{m})(r y - y z_3 - z_2) \\ &\dot{z}_3 = (\omega_c + \beta \hat{m})(y z_2 - b z_3) \\ &\dot{\hat{m}} = K(z_1 - y)\operatorname{sgn}(\psi_1) \\ &\begin{bmatrix} \dot{\psi}_1 \\ \dot{\psi}_2 \\ \dot{\psi}_3 \end{bmatrix} = (\omega_c + \beta \hat{m}) \left(\begin{bmatrix} \sigma & \sigma & 0 \\ 0 & -1 & -y \\ 0 & y & -b \end{bmatrix} + KIr(\mathbf{z}, \psi)\right) \\ &\qquad \times \begin{bmatrix} \psi_1 \\ \psi_2 \\ \psi_3 \end{bmatrix} - \beta \begin{bmatrix} \sigma(z_2 - z_1) \\ r y - y z_3 - z_2 \\ y z_2 - b z_3 \end{bmatrix} \end{aligned} \tag{38}$$

where I is the 3×3 identity matrix and

$$r(\mathbf{z}, \psi) = |\psi_1|. \tag{39}$$

The convergence of $\hat{m}$ when $K = 0.02$ and $\beta = 1$ is shown in Fig. 5. The convergence of the state variable z_2 to x_2 and z_3 to x_3 is shown in Fig. 6.

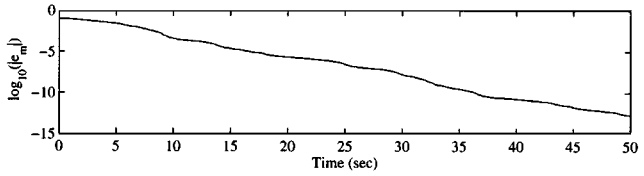

Fig. 5. Convergence of the rate estimate for the Lorenz-based system with $K = 0.02$ and $\beta = 1$.

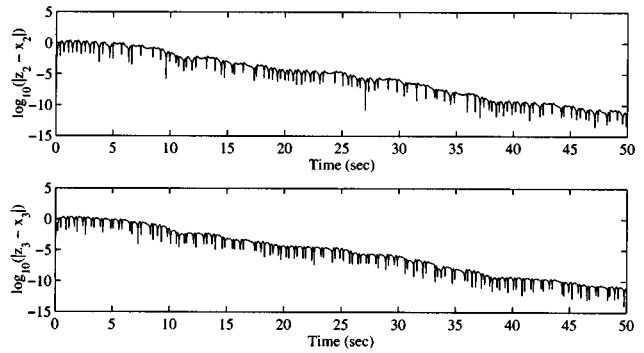

Fig. 6. Convergence of z_2 to x_2 and z_3 to x_3 for the Lorenz-based system with $K = 0.02$ and $\beta = 1$.

V. Demodulator Enhancements

In this section, we explore three modifications that can be made to the demodulator. First, a low-pass filter is added in the feedback path of the rate estimator to remove any spectral energy known to be absent from $m(t)$. Second, the demodulator is modified so that K can be increased beyond K_*, which allows the demodulator to track faster signals. Lastly, the number of nonlinearities present in the rate estimator is reduced by approximating a nonlinear, time-varying component of the rate estimator with a linear, time-invariant system.

A. Filtering

As shown in Section III–B, the rate estimator equation is, to first-order

$$\dot{\hat{m}} = -K\left(\frac{\partial h}{\partial \mathbf{z}}(\mathbf{z})\cdot\boldsymbol{\xi}_1\right)\cdot g\left(\frac{\partial h}{\partial \mathbf{z}}(\mathbf{z})\cdot\boldsymbol{\xi}_1\right)(\hat{m}-m). \quad (40)$$

Now, suppose that we have a smoothing operation, denoted as $\langle\cdot\rangle$, given by

$$\langle y(t)\rangle = \int_0^t \psi(t,\tau)y(\tau)\,d\tau, \quad (41)$$

where $\psi(t,\tau)$ is the smoothing kernel. If the support of this kernel is sufficiently small compared to the rate at which m and $\hat{m}$ vary, then

$$\begin{aligned}\dot{\hat{m}} &= -K\left\langle\left(\frac{\partial h}{\partial \mathbf{z}}(\mathbf{z})\cdot\boldsymbol{\xi}_1\right)\cdot g\left(\frac{\partial h}{\partial \mathbf{z}}(\mathbf{z})\cdot\boldsymbol{\xi}_1\right)(\hat{m}-m)\right\rangle \\ &\approx -K\left\langle\left(\frac{\partial h}{\partial \mathbf{z}}(\mathbf{z})\cdot\boldsymbol{\xi}_1\right)\cdot g\left(\frac{\partial h}{\partial \mathbf{z}}(\mathbf{z})\cdot\boldsymbol{\xi}_1\right)\right\rangle(\hat{m}-m).\end{aligned} \quad (42)$$

The addition of a low-pass filter can be advantageous when additive noise is present since it prevents high-frequency noise-induced oscillations from having adverse effects on the rate estimate.

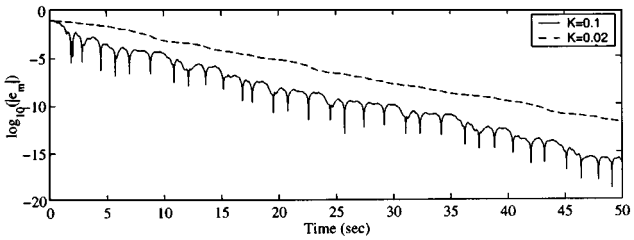

Fig. 7. A comparison of the convergence of $\hat{m}$ when $K = 0.1$ and $K = 0.02$.

Note that the filtering operation described in (41) is not the same filter as the low-pass filter shown in Fig. 2. The filter introduced in (41) is inside the observer/rate estimator feedback loop. The filter shown in Fig. 2 is external to this feedback loop.

B. Increasing the Convergence Rate

In Section III–B, we established a loose upper bound on the rate estimate gain parameter, K, for which the demodulator is stable. From the derivation we see that the convergence of $\hat{m}$ is not only exponential, but also monotonic. By choosing K slightly larger than K_*, monotonic convergence can no longer be guaranteed, but the resulting demodulator may still be stable, as we show with numerical experiments and the circuit described in Section VII. Increasing K has two significant consequences. First, because K governs the rate of convergence of $\hat{m}$, increasing K makes $\hat{m}$ converge faster and allows the demodulator to track signals that vary more rapidly. Second, the perturbation analysis may not be valid because we cannot guarantee that the system will remain stable as K is increased. We can, however, determine, either experimentally or through other numerical techniques such as those based on Floquet theory [6], whether or not the system is stable for a particular value of $K > K_*$.

As an example, we return to the Lorenz system given in (38) and increase K beyond the point at which the perturbation expansion is valid. This requires that the term $KIr(\mathbf{z},\psi)$ be removed from the equation for ψ, otherwise, from the perturbation analysis, we know that the equation governing ψ may be unstable. The demodulator is now given by

$$\begin{aligned}\dot{z}_1 &= (\omega_c+\beta\hat{m})\sigma(z_2-z_1)\\ \dot{z}_2 &= (\omega_c+\beta\hat{m})(ry-yz_3-z_2)\\ \dot{z}_3 &= (\omega_c+\beta\hat{m})(yz_2-bz_3)\\ \dot{\hat{m}} &= K(z_1-y)\operatorname{sgn}(\psi_1)\\ \begin{bmatrix}\dot{\psi}_1\\ \dot{\psi}_2\\ \dot{\psi}_3\end{bmatrix} &= (\omega_c+\beta\hat{m})\begin{bmatrix}\sigma & \sigma & 0\\ 0 & -1 & -y\\ 0 & y & -b\end{bmatrix}\begin{bmatrix}\psi_1\\ \psi_2\\ \psi_3\end{bmatrix}\\ &\quad -\beta\begin{bmatrix}\sigma(z_2-z_1)\\ ry-yz_3-z_2\\ yz_2-bz_3\end{bmatrix}.\end{aligned} \quad (43)$$

The convergence of $\hat{m}$ for $K = 0.1$ and for $K = 0.02$ is shown in Fig. 7. When $K = 0.1, \hat{m}$ repeatedly crosses zero as can be seen in the figure. This cannot happen when $K < K_*$ due to the monotonicity of convergence in that case.

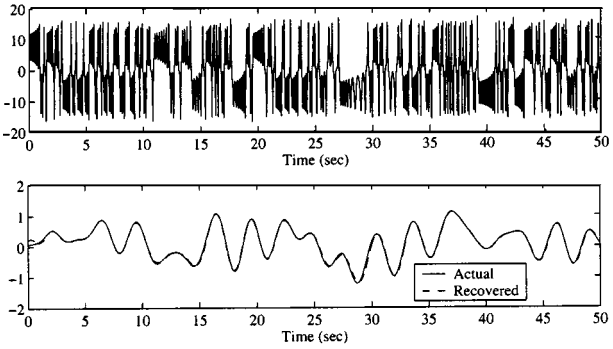

Fig. 8. An example of demodulation. (a) The transmitted signal, $y(t)$. (b) The recovered signal (dashed), the actual modulating signal (solid).

An example of demodulation is shown in Fig. 8. The parameters in this example are $\omega_c = 5, K = 0.6, \beta = 3$, and the modulating signal is a zero-mean Gaussian noise process that has a rectangular power spectral density band-limited to 0.4 Hz and a standard deviation of 0.5.

C. Removal of Some Nonlinearities

The rate estimator contains nonlinearities that appear in the equation for $\boldsymbol{\xi}_1$,

$$\dot{\boldsymbol{\xi}}_1 = \left((\omega_c + \beta\hat{m}) \frac{\partial \hat{\mathbf{f}}}{\partial \mathbf{z}}(\mathbf{z}, y) + KIr(\mathbf{z}, \boldsymbol{\xi}_1) \right) \boldsymbol{\xi}_1 - \beta \hat{\mathbf{f}}(\mathbf{z}, y) \tag{44}$$

where

$$r(\mathbf{z}, \boldsymbol{\xi}_1) = \left(\frac{\partial h}{\partial \mathbf{z}}(\mathbf{z}) \cdot \boldsymbol{\xi}_1 \right) \cdot g\left(\frac{\partial h}{\partial \mathbf{z}}(\mathbf{z}) \cdot \boldsymbol{\xi}_1 \right) \tag{45}$$

$0 < K < K_*$ for some K_*, and $g : \mathbb{R} \to \mathbb{R}$ such that $\operatorname{sgn}(g(a)) = \operatorname{sgn}(a)$. Even when $K > K_*$ and $KIr(\mathbf{z}, \boldsymbol{\xi}_1)$ is removed, a nonlinear equation remains.

The last term in (44), $\beta\hat{\mathbf{f}}(\mathbf{z}, y)$, is generally nonlinear, but it is required by the observer portion of the demodulator. Since this term is already present in the demodulator, removing it from (44) does not reduce the number of nonlinearities. This term is left as it is. The first term in (44), $(\omega_c + \beta\hat{m})(\partial \hat{\mathbf{f}}/d\mathbf{z}) \cdot \boldsymbol{\xi}_1$, is generally nonlinear and does not appear elsewhere in the demodulator. By approximating this term with a linear, time-invariant system, the hardware design discussed in Section VII is greatly simplified.

First, we assume that $\omega_c \gg \beta\hat{m}$ and remove the term $KIr(\mathbf{z}, \boldsymbol{\xi}_1)$ as described in Section V-B. Then (44) becomes

$$\dot{\boldsymbol{\xi}}_1 \approx \omega_c \frac{\partial \hat{\mathbf{f}}}{\partial \mathbf{z}} \boldsymbol{\xi}_1 - \beta \hat{\mathbf{f}}(\mathbf{z}, y). \tag{46}$$

The matrix $(\partial \hat{\mathbf{f}}/d\mathbf{z})(\mathbf{z}, y)$ is generally nonlinear and time-varying. However, (46) is a linear ordinary differential equation and corresponds to a time-varying linear filter with $-\beta\hat{\mathbf{f}}(\mathbf{z}, y)$ as the input. Using the notation $\langle \cdot \rangle$ to denote the filtering operation, (46) becomes

$$\boldsymbol{\xi}_1 = -\beta \langle \hat{\mathbf{f}}(\mathbf{z}, y) \rangle. \tag{47}$$

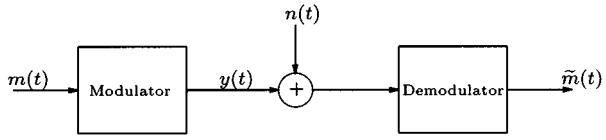

Fig. 9. Additive-noise communication model.

The difference between the derivatives of $\hat{y}$ and y can be approximated as

$$\begin{aligned} \dot{\hat{y}} - \dot{y} &= (\omega_c + \beta\hat{m}) \frac{\partial h}{\partial \mathbf{z}}(\mathbf{z}) \hat{\mathbf{f}}(\mathbf{z}, y) - (\omega_c + \beta m) \frac{\partial h}{\partial \mathbf{z}}(\mathbf{x}) \hat{\mathbf{f}}(\mathbf{x}, y) \\ &= -e_m \beta \frac{\partial h}{\partial \mathbf{z}}(\mathbf{z}) \hat{\mathbf{f}}(\mathbf{z}, y) + \mathcal{O}\left(e_m^2\right). \end{aligned} \tag{48}$$

Filtering $\dot{\hat{y}} - \dot{y}$ gives

$$\langle \dot{\hat{y}} - \dot{y} \rangle \approx -\beta \left\langle \frac{\partial h}{\partial \mathbf{z}}(\mathbf{z}) \hat{\mathbf{f}}(\mathbf{z}, y) \right\rangle e_m \tag{49}$$

where we have assumed that e_m varies slowly with respect to the impulse response of the filter for all t. Assuming further that $h(\mathbf{z}) = C^T\mathbf{z}$, (49) becomes[1]

$$\langle \dot{\hat{y}} - \dot{y} \rangle \approx -\beta \langle \hat{\mathbf{f}}(\mathbf{z}, y) \rangle e_m. \tag{50}$$

Setting $\dot{\hat{m}}$ equal to the product of (47) and (50), we have

$$\begin{aligned} \dot{\hat{m}} &= K\beta^2 \langle \dot{\hat{y}} - \dot{y} \rangle \langle \hat{\mathbf{f}}(\mathbf{z}, y) \rangle \\ &\approx -K\beta^2 \langle \hat{\mathbf{f}}(\mathbf{z}, y) \rangle^2 (\hat{m} - m) \\ &= a(t)(\hat{m} - m) \end{aligned} \tag{51}$$

where $a(t)$ is a negative semi-definite function. The approximation in (51) suggests that $\hat{m}$ converges m.

We can now substitute a different filter for $\langle \cdot \rangle$. For example, a low-pass filter, $\langle \cdot \rangle_L$, results in

$$\begin{aligned} \dot{\hat{m}} = K\beta \big(&(\omega_c + \beta\hat{m}) \langle C^T \hat{\mathbf{f}}(\mathbf{z}, y) \rangle_L \\ &- (y - \langle y \rangle_L) \langle C^T \hat{\mathbf{f}}(\mathbf{z}, y) \rangle_L \end{aligned} \tag{52}$$

where we have made use of the fact that $\langle \dot{y} \rangle_L = (y - \langle y \rangle_L)$.

As an example, we return the Lorenz based system. The modulator equations remain the same as those given in (38). The demodulator equations become

$$\begin{aligned} \dot{z}_2 &= (\omega_c + \beta\hat{m})(ry - yz_3 - z_2) \\ \dot{z}_3 &= (\omega_c + \beta\hat{m})(yz_2 - bz_3) \\ \dot{r}_1 &= -\omega_L(r_1 - y) \\ \dot{r}_2 &= -\omega_L(r_2 - \sigma(z_2 - y)) \\ \dot{\hat{m}} &= K\beta\big((\omega_c + \beta\hat{m})r_2 - (y - r_1)\big)r_2 \end{aligned} \tag{53}$$

where ω_L is the cut-off frequency of the low-pass filter, $\langle \cdot \rangle_L$.

VI. Additive Noise

In this section we demonstrate the robustness with respect to additive noise through numerical simulations for a rate modulation-demodulation system based on the chaotic Lorenz system.

[1]If $h(\mathbf{z}) \neq C^T\mathbf{z}$, then a similar result is obtained by changing (47) to $\boldsymbol{\xi}_1 = -\beta \langle (\partial h)/(\partial \mathbf{z})(\mathbf{z}) \hat{\mathbf{f}}(\mathbf{z}, y) \rangle$.

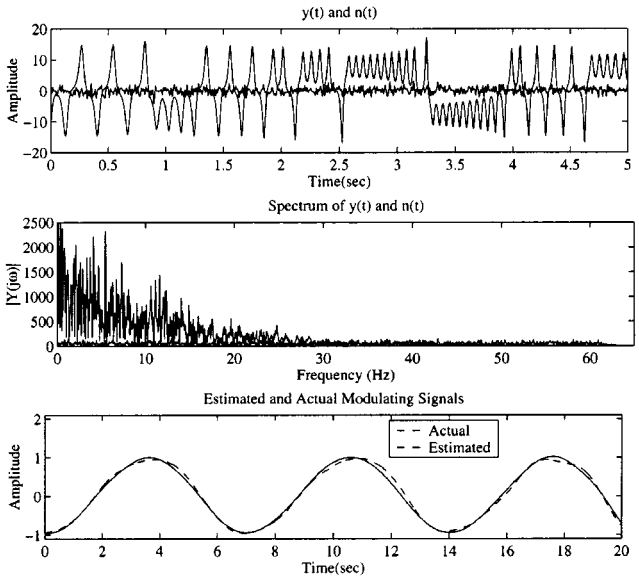

Fig. 10. An example of demodulation in the presence of additive noise.

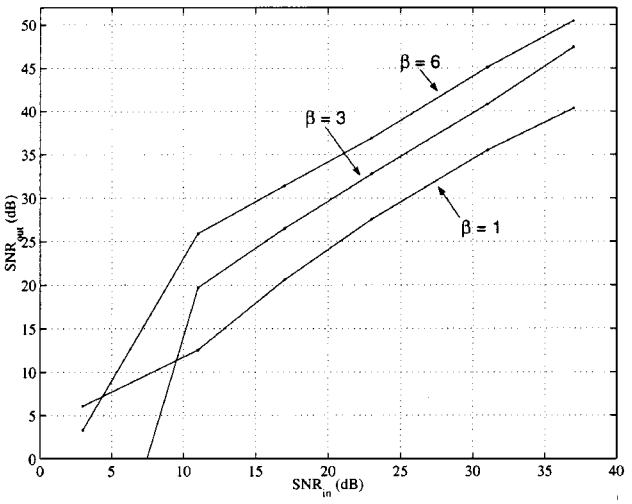

Fig. 11. $\mathrm{SNR_{in}}$ versus $\mathrm{SNR_{out}}$ for several values of β.

Our communication model is shown in Fig. 9. Incorporating the additive noise into the demodulator equations, we get

$$\begin{aligned}\dot{\mathbf{z}} &= (\omega_c + \beta\hat{m})\hat{\mathbf{f}}(\mathbf{z}, y+n)\\ \dot{\hat{m}} &= -K(\hat{y} - (y+n))g\left(\frac{\partial h}{\partial \mathbf{z}}\boldsymbol{\xi}_1\right)\\ \dot{\boldsymbol{\xi}}_1 &= \left((\omega_c + \beta\hat{m})\frac{\partial \hat{\mathbf{f}}}{\partial \mathbf{z}}(\mathbf{z}, y+n) + IKr(\mathbf{z}, \boldsymbol{\xi}_1)\right)\boldsymbol{\xi}_1\\ &\quad - \beta\hat{\mathbf{f}}(\mathbf{z}, y+n). \end{aligned} \tag{54}$$

The output of the demodulator, $\tilde{m}(t)$, is obtained by filtering $\hat{m}(t)$ with a low-pass filter.

In the experiments, which are summarized in Figs. 10 and 11, we generated a wide-band Gaussian noise process and numerically integrated the demodulator system given in (54). Fig. 11 summarizes the effects on the signal-to-noise (SNR) ratio of varying β. In the figure, the input SNR is the ratio between the transmitted signal power and the noise power. Specifically

$$\mathrm{SNR_{in}} = 10\log_{10}\frac{\overline{y^2}}{\sigma_n^2} \tag{55}$$

where σ_n^2 is the variance of the noise process. Similarly, the output SNR is

$$\mathrm{SNR_{out}} = 10\log_{10}\frac{\overline{\hat{m}^2}}{\overline{(\hat{m}-m)^2}}. \tag{56}$$

Two points should be noted. First, there is a SNR gain and, second, there is a trade-off between bandwidth and noise immunity similar to that found in traditional FM.

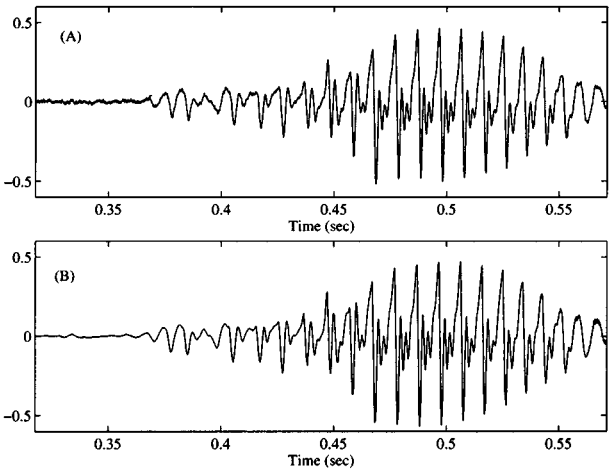

Fig. 12. An example of demodulation. (a) Circuit output. (b) Original speech waveform.

VII. Hardware Implementation

A modulator and demodulator based on the chaotic Lorenz system were implemented in hardware. The circuit design is based on the modulator equations given in (38) and the demodulator equations given in (53). The state variables are rescaled so that their values stay within the operating range of the system components. The rescaled Lorenz equations are

$$\begin{aligned}\dot{X}_1 &= \sigma(X_2 - X_1)\\ \dot{X}_2 &= rX_1 - \frac{9}{2}X_1X_3 - X_2\\ \dot{X}_3 &= \frac{8}{9}X_1X_2 - bX_3 \end{aligned} \tag{57}$$

where σ, r, and b are 10, 25, and $8/3$, respectively.

The differential equations corresponding to the modulator and demodulator are implemented directly in hardware. Specifically, the product of two signals, for example X_1X_3, is obtained using an AD734, which is an analog multiplier made by analog devices. The differential equations are integrated using a standard analog integrator configuration. The operational amplifiers used are OP467s, also made by analog devices. The prototype circuit was etched on doubled sided circuit board. Using a double sided circuit board added design constraints that effect the performance of the circuit. For example, we were unable to

have solid power and ground planes and had to break several traces to route the connections. Using a multilayer circuit board would eliminate these constraints and improve the performance of the circuit. The modulator circuit board measures 6 cm by 10 cm and the demodulator circuit measures 8 cm by 10 cm. The resistors have a 1% tolerance and are surface mount components. The capacitors have a 2.5% tolerance and are polypropylene film capacitors. The component values were chosen so that $\omega_c \approx 100\,000$ and $\beta \approx 18\,000$. The amplitude of the modulating signal, $m(t)$, is assumed to vary 0.2 V peak-to-peak.

Fig. 12 shows a demodulated speech waveform and the original speech waveform of an utterance of the word "this".

VIII. Conclusion

In this paper, we have presented a generalization of frequency modulation in which the carrier waveforms are those generated by a class of dynamical systems. The requirements on the dynamical system are that it has a periodic, almost periodic, or chaotic attractor and that it has a known exponentially convergent observer. Given a dynamical system that meets these requirements, we developed a general and systematic procedure for constructing demodulators. Examples of the modulation scheme were given for the cases in which the underlying dynamical systems were the Van der Pol oscillator and the Lorenz system. We also numerically demonstrated robustness in the presence of additive noise and demonstrated the hardware implementation of the chaotic Lorenz-based modulator and demodulator.

References

[1] A. Volkovskii, "Synchronization of chaotic systems using phase control," *IEEE Trans. Circuits Syst. I*, vol. 44, Oct. 1997.

[2] L. M. Pecora and T. L. Carroll, "Synchronization in chaotic systems," *Phys. Rev.Lett.*, vol. 64, no. 8, pp. 821–824, 1990.

[3] H. K. Khalil, *Nonlinear Systems*, 2nd ed. Upper Saddle River, NJ: Prentice-Hall, 1996.

[4] W. J. Rugh, *Linear System Theory*, 2nd ed. Upper Saddle River, NJ: Prentice-Hall, 1996.

[5] A. Wolf, J. B. Swift, H. L. Swinney, and J. A. Vastano, "Determining Lyapunov exponents from a time series," *Physica D*, vol. 16D, no. 3, pp. 285–317, 1985.

[6] D. W. Jordan and P. Smith, *Nonlinear Ordinary Differential Equations: An Introduction to Dynamical Systems*. New York: Oxford Univ. Press, 1999.

Wade P. Torres (S'98) received the B.S. degree in electrical engineering and the B.S. degree in mathematics from Southern Illinois University at Carbondale, in 1995, and the M.S. degree in electrical engineering from the Massachusetts Institute of Technology (MIT), Cambridge, in 1997. He is currently working toward the Ph.D. degree at MIT in the Digital Signal Processing Group.

From 1995 to 1997, he was with MIT Lincoln Laboratory, Lexington, where he worked on time-frequency analysis of nonstationary signals. Since 1997, he has been with the Digital Signal Processing Group, MIT. He will be joining Bose Corporation after completing his doctoral program. His current research interests are the signal processing aspects of nonlinear dynamical systems and chaos.

Mr. Torres is a member of Sigma Xi and Tau Beta Pi.

Alan V. Oppenheim (F'77) received the S.B. and S.M. degrees in 1961, and the Sc.D. degree in 1964, all in electrical engineering, from the Massachusetts Institute of Technology (MIT), Cambridge, and the honorary doctorate degree from Tel-Aviv University, Tel-Aviv, Israel, in 1995.

In 1964, he joined the faculty at MIT, where he is currently the Ford Professor of Engineering and MacVicar Faculty Fellow with the Department of Electrical Engineering and Computer Science. Since 1967, he as also been affiliated with MIT Lincoln Laboratory, Lexington, and, since 1977, with the Woods Hole Oceanographic Institution, Woods Hole, MA. His research interests are in the general area of signal processing and its applications.

He is coauthor of the widely used textbooks *Discrete-Time Signal Processing* and *Signals and Systems*. He is also Editor of several advanced books on signal processing. Dr. Oppenheim is a member of the National Academy of Engineering and a member of Sigma Xi and Eta Kappa Nu. He has been a Guggenheim Fellow and a Sackler Fellow at Tel-Aviv University. He has also received a number of awards for outstanding research and teaching including the IEEE Education Medal, the IEEE Centennial Award, the Society Award, the Technical Achievement Award, and the Senior Award of the IEEE Society on Acoustics, Speech, and Signal Processing. He has also received a number of awards at MIT for excellence in teaching, including the Bose Award and the Everett Moor Baker Award.

Rodolfo Ruben Rosales received the licenciado degree in mathematics, from the University of Córdoba, Córdoba, Argentina, and the Ph.D. degree in applied mathematics from the California Institute of Technology, Pasadena, in 1973 and 1977, respectively.

He was with University of California at Berkeley, and at the Courant Institute of Mathematical Sciences. In 1979, he joined the faculty at Massachusetts Institute of Technology, Cambridge, MA, where he is now Professor of applied mathematics. His research interests are in nonlinear waves and oscillations.

He received an Alfred P. Sloan Research Fellowship in 1984.